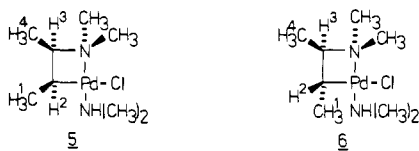


Table I. ^1H and ^{13}C NMR Shifts for the Amination Products^a


	^1H NMR	
H ¹	0.83 (d, $J_{1-2} = 7.3$ Hz)	0.70 (d, $J_{1-2} = 6.4$ Hz)
H ²	1.11 (m, $J_{2-3} = 8.9$ Hz)	0.52 (m, $J_{2-3} = 9.4$ Hz)
H ³	4.16 (m)	3.62 (m)
H ⁴	0.99 (d, $J_{3-4} = 7.1$ Hz)	0.93 (d, $J_{3-4} = 6.7$ Hz)
H ₃ C-N	2.3-2.6	2.3-2.5
	^{13}C NMR	
C ¹	11.95	14.44
C ²	-3.12	0.90
C ³	76.64	81.38
C ⁴	15.94	18.71
H ₃ C-N	42.2-50.0	41.6-49.5

^a Expressed as δ relative to Me_4Si .

B-VT-1000 temperature-control unit. The shifts are expressed as δ relative to Me_4Si . Tetrahydrofuran (THF) was distilled from potassium-benzophenone prior to use. THF- d_6 and methanol- d_4 (Stohler Isotope Chemicals) were taken from freshly opened ampules and used as received.

^{13}C NMR Procedure. Bis(benzonitrile)palladium dichloride (192 mg, 0.50 mmol) was dissolved in 2 mL of THF in a 10-mm NMR tube. The NMR tube was cooled by immersion into a tube containing finely crushed dry ice, and (*E*)-2-butene (34 mL, ca 1.5 mmol) was added from a syringe under stirring with a vortex stirrer. The NMR tube was allowed to warm to ca. -10°C and then cooled to about -78°C , and gaseous dimethylamine (56 mL, ca. 2.5 mmol) was slowly added from a syringe. With stirring the temperature was increased and held at ca. -35°C for a few minutes to ensure complete formation of cyclic chloro(dimethylamino)[*erythro*-3-(*N,N*-dimethylamino)but-2-yl-*C,N*]palladium(II) (**5**). After addition of 0.5 mL of methanol- d_4 that was used to achieve internal lock, the NMR spectrum was recorded at 223 K. With use of the same procedure, (*Z*)-2 butene was converted to chloro(dimethylamino)[*threo*-3-(*N,N*-dimethylamino)but-2-yl-*C,N*]palladium(II) (**6**). The ^{13}C NMR data are presented in Table I.

^1H NMR Procedure. The cyclic complexes were prepared in the same way as described for the ^{13}C NMR except that the scale was decreased to one-tenth, that is 19.2 mg (0.05 mmol) of bis(benzonitrile)palladium dichloride was used, that was dissolved in 0.7 mL of THF- d_6 in a 5-mm NMR tube. The ^1H NMR data are presented in Table I.

Acknowledgment. We thank the Swedish Board for Technical Development and the Swedish Natural Science Research Council for financial support and Professor L. S. Hegedus for helpful discussions.

Registry No. **5**, 91409-21-1; **6**, 91464-43-6; (*E*)-2-butene, 624-64-6; (*Z*)-2-butene, 590-18-1; bis(benzonitrile)palladium chloride, 14220-64-5; dimethylamine, 124-40-3.

Chromium, Molybdenum, and Tungsten Chlorophosphazenes: Molecular Structures of $\text{N}_3\text{P}_3\text{Cl}_5[\text{Cr}(\text{CO})_3(\eta\text{-C}_5\text{H}_5)]$ and $\text{N}_3\text{P}_3\text{Cl}_4(\text{C}_5\text{H}_5)[\text{Mo}(\text{CO})_3(\eta\text{-C}_5\text{H}_5)]$ ^{1,2}

Harry R. Allcock,* Geoffrey H. Riding, and Robert R. Whittle

Contribution from the Department of Chemistry, The Pennsylvania State University, University Park, Pennsylvania 16802. Received November 3, 1983

Abstract: Cyclopentadienylchromium tricarbonyl anion reacts with hexachlorocyclotriphosphazene, $(\text{NPCl}_2)_3$, to form a metallophosphazene of formula $\text{N}_3\text{P}_3\text{Cl}_5[\text{Cr}(\text{CO})_3(\eta\text{-C}_5\text{H}_5)]$ (**5**). The reactions of the analogous molybdenum and tungsten anions with $(\text{NPCl}_2)_3$ are more complex and lead to the formation of metallophosphazenes of formula $\text{N}_3\text{P}_3\text{Cl}_4(\text{C}_5\text{H}_5)[\text{M}(\text{CO})_3(\eta\text{-C}_5\text{H}_5)]$ (**6a**, $\text{M} = \text{Mo}$; **6b**, $\text{M} = \text{W}$) in which the chlorine atom geminal to the metal has been replaced by a cyclopentadiene group. A key requirement for the success of these reactions is the use of a tetra-*n*-butylammonium counterion. The products are among the first chlorophosphazenes to contain metal-phosphorus side-group bonds. The structures of **5** and **6a** were examined in detail by spectroscopic and X-ray diffraction techniques. In both compounds the N-P-N bond angle at the metal-bearing phosphorus is unusually narrow, being $112.3(3)^\circ$ in **5** and $111.0(3)^\circ$ in **6a**. Moreover, an alternation of longer and shorter bond lengths is found for the P-N bonds located at increasing distances from the metal. For **5**, the phosphazene ring was found to be significantly nonplanar. These features are compatible with appreciable interaction between the metal and the phosphorus-nitrogen ring. Crystal data: crystals of **5** are monoclinic with the space group $P2_1/m$ and with $a = 8.334(3)$ Å, $b = 12.897(8)$ Å, $c = 8.783(4)$ Å, $\beta = 105.44(3)^\circ$, $V = 909.9(15)$ Å³, and $Z = 2$; crystals of **6a** are orthorhombic with the space group $Pca2_1$ and with $a = 16.075(3)$ Å, $b = 8.832(3)$ Å, $c = 14.780(3)$ Å, $V = 2098(1)$ Å³, and $Z = 4$.

An expanding interest exists in transition-metal derivatives of the main group inorganic rings, cages, and high-polymeric chains. Part of this interest reflects a search for new catalytic or electroactive materials. One of the largest classes of inorganic rings and chains is the phosphazene system,³ which has been investigated broadly with respect to organic-type substitution processes. By contrast, few transition-metal derivatives of

phosphazenes are known although, in theory, this interfacial area offers much promise for pioneering synthesis, understanding of structural problems, and the discovery of new phenomena.

Recent attempts have been made to link transition metals to phosphazene rings or high polymers by the use of the electron-donor coordination properties of the skeletal nitrogen atoms (**1**)⁴⁻⁹

(1) This work was presented at the 186th National Meeting of the American Chemical Society, Washington, D.C., August 30, 1983.

(2) For a previous paper see: Allcock, H. R.; Lavin, K. D.; Riding, G. H.; Suszko, P. R.; Whittle, R. R. *J. Am. Chem. Soc.* **1984**, *106*, 2337.

(3) Allcock, H. R. "Phosphorus-Nitrogen Compounds"; Academic Press: New York, 1972.

(4) Trotter, J.; Whitlaw, S. R. *J. Chem. Soc. A*, **1970**, 455.

(5) Allcock, H. R.; Allen, R. W.; O'Brien, J. P. *J. Am. Chem. Soc.* **1977**, *99*, 3984, 3987.

(6) Marsh, W. C.; Paddock, N. L.; Stewart, C. J.; Trotter, J. *J. Chem. Soc., Chem. Commun.* **1970**, 1190.

(7) Trotter, J.; March, W. C. *J. Chem. Soc. A*, **1971**, 1482.

(8) Highes, J.; Wiley, C. H. *J. Am. Chem. Soc.* **1973**, *95*, 8758.

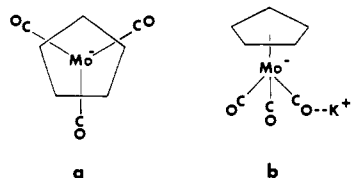
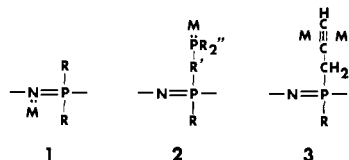


Figure 1. Geometry of the $M(\text{CO})_3(\eta\text{-C}_5\text{H}_5)$ anion in the presence of the $(\text{C}_4\text{H}_9)_4\text{N}$ cation.

or via pendent phosphino^{10,11} (**2**), or propynyl (**3**) units^{12,13} attached to organic side groups. Metal coordination to nido-carborane units attached to a phosphazene ring or chain has also been accomplished.¹⁴ Some evidence for π -complex formation between metals and the phosphazene ring has been reported.^{5,15} However, the



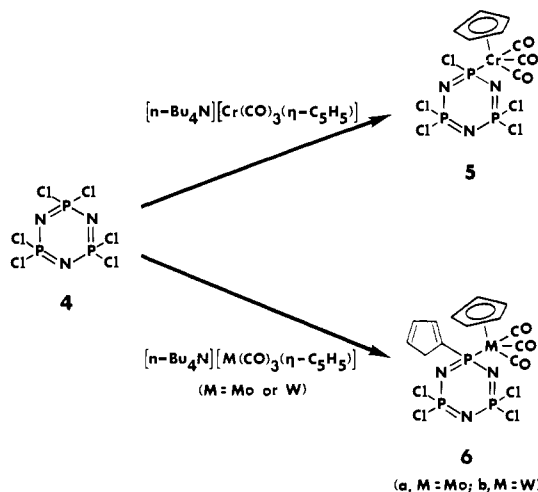
most intriguing objective is the prospect that metallophosphazenes can be prepared in which the transition metal is bonded covalently to the phosphorus atom. The prospect that strong interactions might exist between the metal and the π -electrons of the phosphazene skeleton is of no small interest.

In earlier papers¹⁶⁻¹⁸ we reported the first example of compounds of this type. However, the synthetic route used in that work required the use of fluorophosphazenes as substrates for nucleophilic attack by organometallic anions of iron or ruthenium. A problem with that route is the difficulty involved in extending these reactions to high-polymeric phosphazenes, because fluorophosphazene high polymers can be handled only with difficulty.¹⁹ Most phosphazene high-polymer chemistry is derived from poly(dichlorophosphazene), $(\text{NPCl}_2)_n$. However, in general, organometallic anions react with chlorophosphazenes by halogen abstraction as well as by substitution.

Results and Discussion

The Overall Reaction. In the presence of a tetrabutylammonium counterion to prevent or reduce ion-pair formation, group 6 transition-metal carbonyl anions of the formula $[M(\text{CO})_3(\eta\text{-C}_5\text{H}_5)]^-$ ($M = \text{Cr}, \text{Mo}, \text{or W}$) react with hexachlorocyclo-triphosphazene, $(\text{NPCl}_2)_3$, with attachment of the metal to a phosphorus atom of the ring.

With the chromium anion, a seemingly simple nucleophilic substitution process occurs to yield metallophosphazene **5**. However, with the molybdenum or tungsten anions, the reaction products contain species of type **6**, in which a cyclopentadiene group as well as the metal are covalently attached geminally to a phosphorus atom of the ring. Both **6a** and **6b** were obtained



as pale yellow crystals in moderately good yields (**6a** = 48%, **6b** = 60%, based on the total number of cyclopentadienyl units in the system). Both compounds are stable in air for a short time in the crystalline state but decompose on exposure to light. X-ray structure solutions of **5** and **6a** have been carried out and are discussed later.

Additional products from the reactions of the molybdenum and tungsten organometallic anions were $\text{MoCl}(\text{CO})_3(\eta\text{-C}_5\text{H}_5)$ and $\text{WCl}(\text{CO})_3(\eta\text{-C}_5\text{H}_5)$ (10–15% yields). These compounds were the only products isolated when the potassium salts of $[\text{Mo}(\text{CO})_3(\eta\text{-C}_5\text{H}_5)]^-$ or $[\text{W}(\text{CO})_3(\eta\text{-C}_5\text{H}_5)]^-$ interacted with **4**.²⁰

Clearly, these reactions follow a complex mechanism that involves both halogen abstraction and/or substitution. In the following section we propose mechanistic pathways that seem to account for the data.

Role Played by the Cation. In the absence of a bulky alkylammonium cation, the reaction is quite different. The potassium salt of $[M(\text{CO})_3(\eta\text{-C}_5\text{H}_5)]^-$ ($M = \text{Mo or W}$) reacts with $(\text{NPCl}_2)_3$ to give mainly low yields (10–15%) of the halogen-abstraction products, $\text{MCl}(\text{CO})_3(\eta\text{-C}_5\text{H}_5)$.

We believe that the striking difference between the behavior of the potassium and tetra-*n*-butyl ammonium salts of these organometallic species toward $(\text{NPCl}_2)_3$ is a result of the greater ion-pair separation when the bulkier cation is present. This view is supported by the spectrum of $n\text{-Bu}_4\text{N}[M(\text{CO})_3(\eta\text{-C}_5\text{H}_5)]$ in tetrahydrofuran. The spectrum contains two carbonyl bands at 1896 (s) and 1775 cm^{-1} . This indicates that the carbonyl groups possess pseudo- $C_{3v}(3m)$ symmetry, as shown in Figure 1a. The same symmetry is also seen in the solid state²² and is a result of negligible interaction between the two bulky ions. By contrast, the infrared spectrum of $\text{K}[M(\text{CO})_3(\eta\text{-C}_5\text{H}_5)]$ in tetrahydrofuran shows three carbonyl bands at 1901 (s), 1796, and 1748 cm^{-1} , which is indicative of $C_s(m)$ symmetry and a corresponding inequivalence of the carbonyl ligands. This change is attributed to a close association of the potassium ion with a carbonyl ligand of the anion (Figure 1b). These observations are consistent with the conclusions reported recently by Darensbourg and co-workers.²³ Thus, the presence of an unhindered cation and a close ion pair appears to allow metal-halogen exchange to occur more readily.

Reaction Mechanisms. It appears from the products obtained and from "trapping" experiments using methyl iodide (see later) that the reaction pathway for the chromium anion is significantly different from that for the molybdenum and tungsten anions.

(20) $\text{CrCl}(\text{CO})_3(\eta\text{-C}_5\text{H}_5)$ is apparently unstable.²¹ This may explain why this product was not detected when $\text{K}^+[\text{Cr}(\text{CO})_3(\eta\text{-C}_5\text{H}_5)]^-$ reacts with $(\text{NPCl}_2)_3$ in THF. In the absence of the tetra-*n*-butylammonium salt all three organometallic anions are insoluble in methylene chloride. However, they are soluble in THF.

(21) Manning, A. R.; Thornhill, D. J. *J. Am. Chem. Soc.* **1971**, *93*, 637.
(22) Crotty, D. E.; Corey, R.; Anderson, T. J.; Glick, N. D.; Oliver, J. P. *Inorg. Chem.* **1977**, *16*, 920.

(23) Darensbourg, M. Y.; Jimenez, P.; Skakett, J. R.; Hanekel, J. M.; Kump, R. L. *J. Am. Chem. Soc.* **1982**, *104*, 1521.

(9) Hota, H. K.; Harris, R. O. *J. Chem. Soc., Chem. Commun.* **1972**, 407.
(10) Evans, T. L.; Fuller, T. J.; Allcock, H. R. *J. Am. Chem. Soc.* **1979**, *101*, 262.

(11) Allcock, H. R.; Lavin, K. D.; Tollefson, N. M.; Evans, T. L. *Organometallics* **1983**, *2*, 267.

(12) Allcock, H. R.; Harris, P. J.; Nissan, R. A. *J. Am. Chem. Soc.* **1981**, *103*, 2256.

(13) Allcock, H. R.; Nissan, R. A.; Harris, P. J.; Whittle, R. R. *Organometallics* **1984**, *3*, 432.

(14) Allcock, H. R.; Scopelianos, A. G.; Whittle, R. R.; Tollefson, N. M. *J. Am. Chem. Soc.* **1983**, *105*, 1316.

(15) Cotton, F. A.; Rusholme, G. A.; Shaver, A. *J. Coord. Chem.* **1973**, *99*.

(16) Greigiger, P. P.; Allcock, H. R. *J. Am. Chem. Soc.* **1979**, *101*, 2492.

(17) Allcock, H. R.; Greigiger, P. P.; Wagner, L. J.; Bernheim, M. Y. *Inorg. Chem.* **1981**, *20*, 716.

(18) Allcock, H. R.; Wagner, L. J.; Levin, M. L. *J. Am. Chem. Soc.* **1983**, *105*, 1321.

(19) Allcock, H. R.; Evans, T. L.; Patterson, D. B. *Macromolecules* **1980**, *13*, 201.

Table I. NMR Spectral Data for **5**, **6a**, **6b**, and **10**

	$^1\text{H}^a$	$^{13}\text{C}^a$	$^{31}\text{P}^a$
5	5.29 (C ₅ H ₅) (d, $J_{\text{PCrCH}} = 1.5$ Hz)	220.6 (s), 219.2 (s), 214.1 (d, $J_{\text{PCrC}} = 22$ Hz), (Cr-CO), 92.7 (s) (CrC ₅ H ₅)	140.3 (t) (P _{ClCr}), 12.6 (d) (P _{Cl₂}) ($J_{\text{PNP}} = 88$ Hz)
6a	6.93 (m, 1 H), 6.69 (m, 1 H), 6.52 (m, 1 H), 5.60 (d, $J_{\text{PMoCH}} = 0.6$ Hz, 5 H), 3.36 (m, 2 H)	140.2 (d, $J_{\text{PC}} = 14.8$ Hz), 138.4 (d, $J_{\text{PC}} = 7.4$ Hz), 131.5 (d, $J_{\text{PC}} = 15.7$ Hz), 95.2 (s), 42.5 (d, $J_{\text{PC}} = 13.0$ Hz)	86.02 (t) (P _{CpMo}), 9.04 (d) (P _{Cl₂}) ($J_{\text{PNP}} = 49$ Hz)
6b	6.91 (m, 1 H), 6.69 (m, 1 H), 6.53 (m, 1 H), 5.71 (d, $J_{\text{PW}} = 0.8$ Hz, 5 H), 3.34 (m, 2 H)	140.5 (d, $J_{\text{PC}} = 14.8$ Hz), 138.4 (d, $J_{\text{PC}} = 7.8$ Hz), 131.4 (d, $J_{\text{PC}} = 16.5$ Hz), 94.0 (s), 42.5 (d, $J_{\text{PC}} = 12.9$ Hz)	58.5 (d) (P _{CpW}), 12.4 (d) (P _{Cl₂}) ($J_{\text{PNP}} = 48$ Hz)
10	5.71 (s, 5 H), 2.14 (d, t, $J_{\text{PCH}} = 9.8$ Hz, $J_{\text{PNPCH}} = 1.3$ Hz)		58.9 (t) (P _{MeW}), 8.8 (d) (P _{Cl₂}) ($J_{\text{PNP}} = 39$ Hz)

The reaction between the chromium anion and (NPCL₂)₃ appears to proceed via a simple nucleophilic attack by the anion on the phosphazene to yield **5**.

By contrast, both substitution and metal-halogen exchange take place when the molybdenum and tungsten anions react with (NPCL₂)₃. Two plausible pathways that lead to a key organometallic intermediate, **9**, are illustrated in Scheme I. The first involves an initial nucleophilic replacement of chlorine to yield **7**, followed by metal-halogen exchange with the geminal chlorine atom to yield **9**. The second alternative involves an initial metal-halogen exchange process between (NPCL₂)₃ and the metallo anion to yield ionic intermediate **8**. Substitution at the tricoordinate phosphorus would then give **9**.

The subsequent reactions of **9** determine the nature of the final products. With the tungsten and molybdenum systems, these final reactions appear to proceed by a nucleophilic attack by **9** on a cyclopentadienyl metallo species in solution, followed by both loss of the metal and a 1,2-hydrogen shift.

Of the two pathways proposed that lead to the organometallic intermediate **9**, the one involving substitution first followed by cation-halogen exchange appears unable to account for the formation of **9**. All attempts to generate the chromium analogue of **9** via a cation-halogen exchange with the tungsten anion, and to subsequently trap this intermediate, have failed. Thus, the chromium analogue of **7** was recovered unchanged when treated with [n-Bu₄N][W(CO)₃(η-C₅H₅)] in CH₂Cl₂ solution, either alone or in the presence of WCl(CO)₃(η-C₅H₅) or MeI.

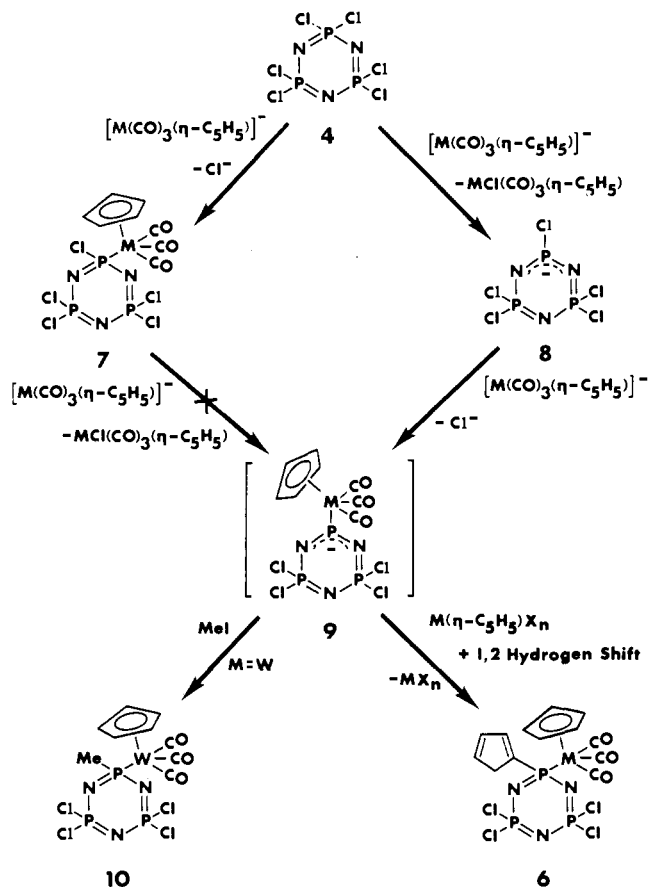
If this mechanism is correct, it raises several questions. (1) What evidence exists that **9** plays a key role in the mechanism? Can **9** be detected or "trapped"? (2) What evidence can be found to support the idea of cation-halogen exchange with R₄N⁺[M(CO)₃(η-C₅H₅)]⁻? For example, can MCl(CO)₃(η-C₅H₅) be detected as a side product? (3) Why does the chromium anion behave differently from the molybdenum and tungsten analogues? (4) What is the mechanism of the curious transformation that yields **6**?

Evidence for the participation of **9** in the molybdenum- and tungsten-type reactions was obtained by the addition of an equimolar amount of methyl iodide to a mixture of Bu₄N[W(CO)₃(η-C₅H₅)] and (NPCL₂)₃ in methylene chloride. This brought about a reduced yield of **6b** and generated a significant quantity of the *gem*-methyl tungsten phosphazene species, **10b**. This compound was not formed by a pathway that involved cation-iodide exchange between R₄N⁺[W(CO)₃(η-C₅H₅)]⁻ because, under carefully controlled conditions, no WI(CO)₃(η-C₅H₅) was detected. Hence the formation of **10b** provides strong evidence for the presence of **9** in the main reaction manifold. Similar intermediates have been proposed for the reactions of (NPCL₂)₃ with Grignard reagents²⁴ or lithiometalloenes.²

Strong confirmation for the metal-halogen exchange process was obtained by the isolation of MoCl(CO)₃(η-C₅H₅) and WCl(CO)₃(η-C₅H₅) from the reaction mixtures.

The striking differences between the reactions of the chromium and molybdenum or tungsten anions seem to reflect differences in the propensity for substitution vs. cation-halogen exchange. All attempts to "trap" the chromium analogue of **9** with the use of methyl iodide failed to yield the analogue of **10**. The only effect of the methyl iodide was to decrease the yield of **5** and generate CrI(CO)₃(η-C₅H₅) in good yield (37%). This is surprising because

Scheme I



a, M = Mo; **b**, M = W

Bu₄N[Cr(CO)₃(η-C₅H₅)] reacts with methyl iodide in the absence of the chlorophosphazene to give good yields of CrCH₃(CO)₃(η-C₅H₅) but no CrI(CO)₃(η-C₅H₅).

Finally, the formation of **6** presents a curious anomaly at two levels. First, it is not clear how a cyclopentadienyl group is abstracted from another molecule in order to generate **6**. And second, the driving force for the 1,2-hydrogen shift within the cyclopentadienyl unit needs to be explained. It could be argued that the 1,2-shifted cyclopentadienyl substituent provides better "resonance" conjugation with the phosphazene ring, but it is doubtful if this would provide a sufficient driving force for the formation of the product.

Spectroscopic Characteristics of 5, 6a, and 6b. The spectroscopic data are summarized in Table I and in the Experimental Section.

The infrared spectrum of **5** contained absorbances for terminal C=O ligands of 2049 (s) and 1977 (s, br) cm⁻¹ (in CH₂Cl₂ solution) that are characteristic of a *fac*-M(CO)₃ unit. Additional absorbances were found at 1174 (s) and 1162 (s) cm⁻¹ (KBr disk) from the P=N stretching modes. The electron impact mass

spectrum of **5** did not show the parent ion. Instead, the parent ion, minus one carbonyl ligand, was detected (m/e 487). However, the elemental microanalysis was compatible with structure **5**. The ^1H NMR spectrum of **5** consisted of a closely spaced doublet at 5.29 ppm (downfield from Me_4Si) assigned to the cyclopentadienyl proton ($J_{\text{PCrCH}} = 1.5$ Hz), and the ^1H -decoupled ^{13}C NMR spectrum contained a sharp singlet at 95.2 ppm (downfield from Me_4Si) attributed to the carbon atoms of the cyclopentadienyl ring. The ^{31}P NMR spectrum revealed a clear AX_2 spin system with peaks at 140.3 ppm (P_{CrCl} as a triplet with $J_{\text{PNP}} = 88$ Hz) and at 12.6 ppm (P_{Cl_2} as a doublet). This low chemical shift position for P_{CrCl} and the high coupling constant are unusual features. A similar phenomena was detected for phosphazenes linked directly to iron atoms.¹⁷

The spectroscopic properties of **6a** and **6b** are similar. Hence, only the molybdenum derivative (**6a**) will be discussed. The infrared spectrum of **6a** contained absorbances for terminal $\text{C}=\text{O}$ ligands 2049 (s) and 1968 (s, br) cm^{-1} (in CH_2Cl_2 solution) that are again characteristic of a *fac*- $\text{M}(\text{CO})_3$ unit. Additional absorbances were found at 1195 (s) and 1150 (m) cm^{-1} (KBr disk) from the $\text{P}=\text{N}$ stretching modes. The electron-impact mass spectrum of **6a** did not show the parent ion. Instead, the parent ion, minus one carbonyl ligand, was observed (m/e 559). The elemental analysis was compatible with structure **6a**.

The ^1H NMR spectrum of **6a** showed resonances for the cyclopentadienyl ring attached to phosphorus and for the π -bonded cyclopentadienyl ring attached to the molybdenum atom. Three multiplets, each having an integrated intensity of 1 H at δ 6.93, 6.69, and 6.57, were assigned to the three inequivalent olefinic-type protons of the P-bonded cyclopentadiene group, and a further multiplet of integrated intensity 2 H at δ 3.36 was assigned to the two hydrogens of the methylene group in the same ring. A closely spaced doublet (integrated intensity, 5 H) was attributed to the five equivalent cyclopentadienyl protons ($J_{\text{PMoCH}} = 0.6$ Hz). The ^1H decoupled ^{13}C NMR spectrum contained resonances only for the carbon atoms bonded to hydrogen. Resonances for the carbonyl carbon atoms and the carbon atom of the cyclopentadiene ring bonded to the phosphazene ring were not found because of the absence of a Nuclear Overhauser effect on these carbon atoms and the low solubility of the compounds. Resonances were detected at δ 140.2 (d, $J_{\text{PC}} = 14.8$ Hz), 138.4 (d, $J_{\text{PC}} = 7.4$ Hz), and 131.5 (d, $J_{\text{PC}} = 15.7$ Hz) for the three olefinic-type CH units of the P-bonded cyclopentadiene ring and at δ 42.5 (d, $J_{\text{PC}} = 13.0$ Hz) for the methylene group. A sharp singlet was also observed at δ 95.2 for the cyclopentadienyl ring attached to molybdenum. The ^1H -decoupled ^{31}P NMR spectrum revealed a clear AX_2 spin system with a triplet centered at δ 86.0 ($J_{\text{PNP}} = 49$ Hz), assigned to the cyclopentadienyl- and molybdenum-substituted phosphorus, and a doublet centered at δ 9.0, assigned to the two equivalent PCl_2 units.

Although the above spectral properties clearly indicate that the structure of **6a** consists of a tetrachlorocyclophosphazene ring bearing a geminal [$\text{Mo}(\text{CO})_3(\eta\text{-C}_5\text{H}_5)$] unit via a molybdenum-phosphorus covalent bond and a cyclopentadiene ring linked to phosphorus through an olefinic carbon-phosphorus bond, it was not possible to distinguish between attachment through the carbon atom adjacent to the methylene group or through one of the distal carbon atoms. To distinguish between these two possible isomers, an X-ray crystal-structure analysis was performed (see later).

The infrared spectrum of **10** contained absorbances for terminal $\text{C}=\text{O}$ ligands at 2035 (s), 1957 (sh), and 1942 (s) cm^{-1} (in CH_2Cl_2 solution). Additional absorbances were found at 1200 (s), 1165 (s), and 1151 (s) cm^{-1} (KBr disk) for the $\text{P}=\text{N}$ stretching modes. The electron-impact mass spectrum again failed to show a parent ion. Instead, the parent ion, minus one carbonyl ligand, was detected (m/e 593). However, the elemental microanalysis was compatible with the proposed structure. The ^1H NMR spectrum consisted of a singlet at δ 5.71 (5 H), assigned to the cyclopentadienyl protons, and a doublet of triplets at δ 2.14 (3 H), assigned to the methyl protons ($J_{\text{PCH}} = 9.8$ Hz, $J_{\text{PNPCH}} = 1.3$ Hz). The ^1H -decoupled ^{31}P NMR spectrum revealed an AX_2 spin system with a triplet centered at δ 58.9, assigned to the meth-

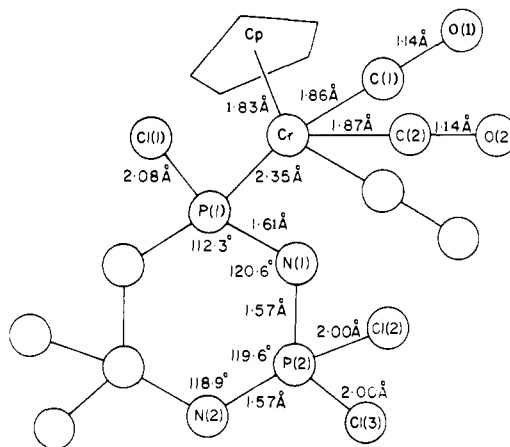


Figure 2. Main structural features of compound **5**.

yl-tungsten-substituted phosphorus, and a doublet at δ 8.8 ($J_{\text{PNP}} = 39$ Hz), assigned to the PCl_2 units.

X-ray Structure of 5. An X-ray single-crystal analysis confirmed that **5** contained a [$\text{Cr}(\text{CO})_3(\eta\text{-C}_5\text{H}_5)$] unit linked to the chlorocyclophosphazene ring through a P-Cr covalent bond. All features of the molecule were identified including the hydrogen atoms attached to the cyclopentadienyl ring. The molecule was found to lie on a mirror plane (at $z = 1/4$), with a plane of symmetry passing through the chromium atom. The main structural features of **5** are summarized in Tables II and III and in Figure 2. A stereo ORTEP view is shown in Figure 3 (supplementary material).

The chromium-phosphorus bond distance is 2.35 Å. The cyclopentadienyl ring is planar and is symmetrically separated from the chromium atom by a distance of 1.83 Å. The average distance between the chromium and carbonyl carbon atoms is 1.865 Å with average carbon-oxygen distances within the carbonyl units of 1.138 Å. All these values are normal. The dihedral angles between the cyclopentadienyl and phosphazene rings is 11.6° , and the carbonyl ligands are essentially colinear with the Cr-C bonds. (The average Cr-C-O angle is 178.5° .)

Perhaps the most unexpected feature of this structure is the nonplanarity of the phosphazene ring (see Figure 4). Atom P(1) is bent approximately 0.27 Å from a plane through the remaining ring atoms. The skeletal distance between P(1) and N(1) is also significantly longer than the other ring distances. Thus, P(1)-N(1) is 1.61 Å and P(2)-N(1) or P(2)-N(2) is 1.57 Å. The N-P-N angle at P(1) is 112.3° , a narrower angle than at the other phosphorus atoms (118.9 – 120.6°) (see Table II). Interestingly, the distance of P(1)-Cl(1) (2.08 Å) is slightly longer than the other P-Cl distances (2.00 Å). This latter value is more typical of those found in a wide range of other chlorophosphazenes.

Thus, the organometallic component has a significant effect on the phosphazene ring, but only in the immediate vicinity of the site of attachment. A study of the nonbonding distances did not reveal any close contacts that would explain these distortions. Hence, we conclude that a distinct electronic interaction exists between the metal and the nearby delocalized π -electrons of the ring. In these terms, it would be of considerable interest to know the effects of nongeminal metal atoms on the structure of the phosphazene ring. However, such derivatives have not yet been isolated.

X-ray Structure of 6a. The X-ray structure analysis of **6a** confirmed that the molecule consists of a chlorocyclophosphazene ring to which a $\text{Mo}(\text{CO})_3(\eta\text{-C}_5\text{H}_5)$ unit and a cyclopentadiene ring are linked in a geminal manner through P-Mo and P-C covalent bonds, respectively. The structure solution also demonstrated clearly that the cyclopentadiene group is linked to the phosphazene ring via the carbon atom adjacent to the methylene group, as illustrated in Tables IV and V and in Figures 5 and 6 (supplementary material).

The coordination about the molybdenum atom is similar to that observed about the chromium atom in **5**. The increases in met-

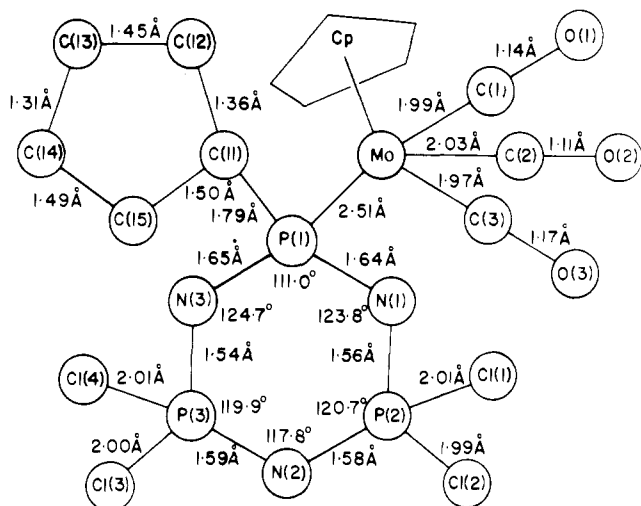


Figure 5. Main structural features of compound 6a.

al-to-ligand bond distances are attributed to the larger covalent radius of Mo(II) compared to Cr(II). The molybdenum-phosphorus bond distance is 2.51 Å. The cyclopentadienyl ring is planar and is separated from the molybdenum atom. The average metal-carbonyl carbon atom distance is 2.00 Å, and the average C-O distance from the carbonyl ligands is 1.141 Å. All these values are normal. The dihedral angle between the cyclopentadienyl ligand and the phosphazene ring is 32°, and the carbonyl ligands are essentially colinear with the Mo-C bonds (the average Mo-C-O angle is 176.5°).

The structural parameters for the P-bonded cyclopentadiene ring are normal. The location of the two double bonds and the shortening of the single bond between them are quite evident. The double bond adjacent to the electron-withdrawing phosphazene ring (length 1.37 Å) was found to be somewhat longer than the other double bonds (length 1.31 Å). The five carbon atoms of the cyclopentadiene ring and the phosphorus atom to which it is attached are coplanar, all six atoms lying within 0.01 Å of the plane. The planes through the cyclopentadiene and phosphazene rings are nearly perpendicular, with a dihedral angle of 87°.

The structure of the phosphazene ring is similar to that found for 5, except that the distortion from planarity of the ring is less severe, atom P(1) being bent only 0.16 Å from a plane through the remaining ring atoms. The skeletal bonds adjacent to the metal are again longer than the other P-N bonds. Similarly, an alternation in longer and shorter bonds exists for the P-N bonds located at increasing distance from this phosphorus atom P(1). Thus, the average length of P(1)-N(1) and P(2)-N(2) is 1.65 Å, P(2)-N(1) and P(3)-N(3) is 1.55 Å, and P(2)-N(2) and P(3)-N(2) is 1.58 Å. This pattern of variation in P-N bond lengths has been observed in other metallophosphazenes. The N-P-N angle at P(1) is 111.0°, a narrower angle than the other ring angles (117.8–124.7°).

Experimental Section

Materials. $[\text{Cr}(\text{CO})_3(\eta\text{-C}_5\text{H}_5)]_2$ and $[\text{W}(\text{CO})_3(\eta\text{-C}_5\text{H}_5)]_2$ were prepared by a published method²⁵ with use of the appropriate metal carbonyl (Strem) and sodium cyclopentadienide. $[\text{Mo}(\text{CO})_3(\eta\text{-C}_5\text{H}_5)]_2$ was prepared by a published method with use of $\text{Mo}(\text{CO})_6$ (Alfa) and dicyclopentadiene (Aldrich)²⁶. $[\text{Mo}(\text{CO})_3(\eta\text{-C}_5\text{H}_5)]_2$ and $[\text{W}(\text{CO})_3(\eta\text{-C}_5\text{H}_5)]_2$ were further purified by recrystallization three times from chloroform. Sodium/potassium alloy was prepared as reported previously from sodium and potassium metal (Fisher).²⁷ Hexachlorocyclotriphosphazene ($\text{N}_3\text{P}_3\text{Cl}_6$) (kindly supplied by Ethyl Corp. and by the Firestone Tire and

Table VI. Summary of Crystal Data and Intensity Collection Parameters

	5	6a	6b
cryst size, mm	0.25 × 0.25 × 0.18	0.10 × 0.30 × 0.29	0.22 × 0.35 × 0.58
fw, amu	513.3	586.9	674.8
space group	$P2_1/m$	$Pca2_1$	$Pca2_1$
a, Å	8.334 (3)	16.075 (3)	16.053 (2)
b, Å	12.897 (8)	8.832 (3)	8.832 (3)
c, Å	8.783 (4)	14.780 (3)	14.755 (4)
β, deg	105.44 (3)		
vol, Å ³	909.9 (15)	2098 (1)	2092 (2)
Z	2	4	4
d(calcd), g/cm ³	1.87	1.86	2.14
d(found), g/cm ³		1.85	2.12
2θ limits	3.0–44.0	3.0–55.8	
scan width (λ + 0.347 tan θ)°	0.80	0.70	
scan rate, deg min ⁻¹	1.0–4.0	1.0–5.0	
no. of unique obsd data (I > 2σ(I))	1214	1864	
μ, cm ⁻¹	16.54	13.58	
R/R _w	0.054/ 0.056	0.041/ 0.043	
esd	2.760	2.219	
data/parameter	9.87	7.63	
drift correction (anisotropic)	1.213	1.037	
av shift/error	0.01	0.06	

Rubber Co.) was purified by recrystallization from hexane and by sublimation, followed by a second recrystallization from hexane. Tetrahydrofuran (Fisher) was dried and distilled from sodium benzophenone ketyl. Dichloromethane (Fisher) and diethyl ether (Baker) were distilled from calcium hydride immediately before use. Column chromatography was performed with silica gel (230–400 mesh ASTM) (Scientific Products). All reactions were performed under an atmosphere of dry nitrogen with standard airless-ware (Kontes).

Equipment. ¹H, ¹³C, and ³¹P NMR spectra were recorded on a Bruker WH 200 NMR spectrometer. The ³¹P shifts are relative to aqueous 85% H₃PO₄, with positive shifts downfield from this reference. Infrared spectra were recorded on a Perkin-Elmer 580 grating spectrophotometer, both in solution in CH₂Cl₂ or as a solid (KBr disk). Electron-impact mass spectral results were obtained with an AEI MS 902 mass spectrometer and were tabulated by a linked computer. Mass spectral isotope patterns were also calculated and tabulated.

Preparation of $[n\text{-Bu}_4\text{N}][\text{Cr}(\text{CO})_3(\eta\text{-C}_5\text{H}_5)]$. The potassium salt $\text{K}[\text{Cr}(\text{CO})_3(\eta\text{-C}_5\text{H}_5)]$ was first prepared by the method of Ellis and co-workers²⁷ with the use of sodium/potassium alloy as a reducing agent. In a typical reaction, a sample of $[\text{Cr}(\text{CO})_3(\eta\text{-C}_5\text{H}_5)]_2$ (3 g, 7.46 mmol) was dissolved in tetrahydrofuran (50 mL). Sodium/potassium alloy (2 mL) was then added via syringe, and the mixture was stirred until the dark green $[\text{Cr}(\text{CO})_3(\eta\text{-C}_5\text{H}_5)]_2$ was reduced to the pale yellow salt, $\text{K}[\text{Cr}(\text{CO})_3(\eta\text{-C}_5\text{H}_5)]$. The solution was filtered to remove the excess alloy, and the solvent was then removed under reduced pressure. A solution of $n\text{-Bu}_4\text{NBr}$ (5 g, 15.53 mmol) in dichloromethane (50 mL) was then added to the pale yellow solid obtained above, and the mixture was stirred. After 30 min, a yellow solution of $[n\text{-Bu}_4\text{N}][\text{Cr}(\text{CO})_3(\eta\text{-C}_5\text{H}_5)]$ and a fine white precipitate of KBr were obtained.

Preparation of $[n\text{-Bu}_4\text{N}][\text{Mo}(\text{CO})_3(\eta\text{-C}_5\text{H}_5)]$ and $[n\text{-Bu}_4\text{N}][\text{W}(\text{CO})_3(\eta\text{-C}_5\text{H}_5)]$. The procedures used for the preparation of these complex salts were similar to those described above for $[n\text{-Bu}_4\text{N}][\text{Cr}(\text{CO})_3(\eta\text{-C}_5\text{H}_5)]$.

Preparation of $\text{N}_3\text{P}_3\text{Cl}_6[\text{Cr}(\text{CO})_3(\eta\text{-C}_5\text{H}_5)]$ (5). A solution of $[n\text{-Bu}_4\text{N}][\text{Cr}(\text{CO})_3(\eta\text{-C}_5\text{H}_5)]$ (14.9 mol) in dichloromethane (50 mL), prepared as described above, was added dropwise to a solution of $(\text{N}_3\text{P}_3\text{Cl}_6)_3$ (6 g, 17.2 mmol) in dichloromethane (50 mL), and the mixture was stirred for 17 h. The solvent was then removed under reduced pressure, and the products were extracted with two 150-mL portions of diethyl ether. The extracts were combined and the solvent was again removed under reduced pressure to give a dark yellow solid. The product was purified by column chromatography on a short silica gel column (3.0 cm × 15 cm). Elution with dichloromethane-hexane (1:5) developed a yellow band, which yielded bright yellow crystals of $\text{N}_3\text{P}_3\text{Cl}_6[\text{Cr}(\text{CO})_3(\eta\text{-C}_5\text{H}_5)]$ (3.2 g, 42%), mp 170 °C dec. Anal. Calcd for $\text{C}_8\text{H}_2\text{O}_3\text{Cl}_3\text{CrN}_3\text{P}_3$: C, 18.70; H, 0.97; Cl, 34.57; N, 8.18; P, 18.11. Found: C, 18.51; H, 1.03; Cl, 34.71; N, 8.09; P, 18.25. Infrared peaks (KBr disk) (cm⁻¹): 2042 (s), 1990 (s), 1965 (s, br) (ν_{CO}); 1174 (s), 1162 (s) (ν_{PN}); (in CH₂Cl₂ solution) 2049 (s), 1977 (s, br) (ν_{CO}).

(24) Allcock, H. R.; Desorcie, J. L.; Harris, P. J. *J. Am. Chem. Soc.* **1983**, *105*, 2814.

(25) Birdwhistell, R.; Hackett, P.; Manning, A. R. *J. Organomet. Chem.* **1978**, *157*.

(26) King, R. B. "Organometallic Synthesis"; Academic Press: New York, 1965, Vol. 1.

(27) Ellis, J. E.; Flom, E. A. *J. Organomet. Chem.* **1975**, *99*, 263.

Table VII. Positional and Thermal Parameters^a and Their Estimated Standard Deviations for **5**

atom	x	y	z	U(1,1)	U(2,2)	U(3,3)	U(1,2)	U(1,3)	U(2,3)
Cr	0.2388 (2)	0.2500 (0)	1.0536 (1)	0.0331 (7)	0.0646 (9)	0.0237 (6)	0	0.0035 (5)	0
Cl1	0.1838 (3)	0.2500 (0)	0.6332 (2)	0.074 (2)	0.085 (2)	0.035 (1)	0	0.021 (1)	0
Cl2	-0.2123 (2)	0.0505 (1)	0.4538 (2)	0.073 (1)	0.070 (1)	0.071 (1)	-0.001 (1)	0.006 (1)	-0.032 (1)
Cl3	-0.4010 (2)	0.0724 (2)	0.7102 (2)	0.060 (1)	0.070 (1)	0.099 (1)	-0.012 (1)	0.0258 (9)	0.010 (1)
P1	0.0496 (3)	0.2500 (0)	0.8019 (2)	0.035 (1)	0.040 (1)	0.030 (1)	0	0.0004 (9)	0
P2	-0.2287 (2)	0.1450 (1)	0.6292 (2)	0.0390 (9)	0.0371 (9)	0.0474 (8)	-0.0046 (9)	-0.0018 (7)	-0.0043 (9)
O1	0.6121 (9)	0.2500 (0)	1.1317 (10)	0.036 (4)	0.23 (1)	0.097 (6)	0	0.003 (4)	0
O2	0.3081 (6)	0.4541 (4)	0.9188 (5)	0.094 (3)	0.088 (3)	0.060 (3)	-0.047 (3)	0.014 (2)	0.001 (3)
N1	-0.0618 (6)	0.1461 (4)	0.7641 (5)	0.038 (3)	0.038 (3)	0.053 (3)	0.000 (3)	-0.008 (2)	-0.000 (3)
N2	-0.3049 (9)	0.2500 (0)	0.5514 (9)	0.050 (5)	0.027 (4)	0.063 (4)	0	-0.019 (4)	0
C1	0.4706 (12)	0.2500 (0)	1.1033 (11)	0.033 (5)	0.15 (1)	0.048 (5)	0	0.000 (5)	0
C2	0.2807 (8)	0.3759 (5)	0.9660 (7)	0.044 (3)	0.071 (4)	0.035 (3)	-0.021 (4)	0.005 (3)	-0.007 (3)
C1P	0.0089 (10)	0.2500 (0)	1.1306 (10)	0.027 (5)	0.18 (1)	0.041 (5)	0	0.017 (4)	0
C2P	0.1035 (9)	0.3372 (6)	1.1927 (8)	0.074 (4)	0.066 (5)	0.059 (3)	0.006 (4)	0.033 (3)	0.004 (4)
C3P	0.2540 (8)	0.3037 (5)	1.2905 (6)	0.073 (4)	0.059 (4)	0.032 (3)	-0.004 (4)	0.014 (3)	-0.012 (3)
H1P	-0.091 (10)	0.250 (0)	1.078 (9)	0.0384 (0)					
H2P	0.077 (7)	0.396 (4)	1.166 (6)	0.0384 (0)					
H3P	0.327 (7)	0.343 (5)	1.342 (6)	0.0384 (0)					

^aThe form of the anisotropic thermal parameter is $\exp[-2\pi^2(U_{11}a^2h^2 + U_{22}b^2k^2 + U_{33}c^2l^2 + 2U_{12}a^*b^*hk + 2U_{13}a^*c^*hl + 2U_{23}b^*c^*kl)]$.

Preparation of $N_3P_3Cl_4(C_5H_5)[Mo(CO)_3Co(\eta-C_5H_5)]$ (6a**).** A solution of [*n*-Bu₄N][Mo(CO)₃(η -C₅H₅)] (8.16 mmol), prepared as described above, was added dropwise to a solution of (NPCl₂)₃ (3.5 g, 10.0 mmol) in dichloromethane (50 mL) and stirred for 2 h at room temperature. The reaction solvent was then removed under reduced pressure, and the products were separated by column chromatography. Elution with dichloromethane-hexane (1:4) gave an orange band of Mo(CO)₃Cl(η -C₅H₅) (360 mg), identified by comparison of its carbonyl IR spectrum with that of an authentic sample. Further elution with dichloromethane-hexane (1:1) gave a pale yellow band from which pale yellow crystals of N₃P₃Cl₄(C₅H₅)[Mo(CO)₃(η -C₅H₅)] (**6a**) (1.10 g, 48%) were obtained, mp 210 °C dec. Anal. Calcd for C₁₃H₁₀N₃Cl₄MoO₃P₃: C, 26.58; H, 1.70; Cl, 24.16; N, 7.15; P, 15.85. Found: C, 25.54; H, 1.78; Cl, 25.15; N, 7.07; P, 15.99. Infrared peaks (KBr disk) (cm⁻¹): 2042 (s), 1976 (s), (ν_{CO}); 1195 (s), 1150 (m) (ν_{PN}); 517 (s), 457 (m), 416 (s) (ν_{PCl}); (in CH₂Cl₂ solution) 2045 (s), 1968 (s, br) (ν_{CO}).

Preparation of $N_3P_3Cl_4(C_5H_5)[W(CO)_3(\eta-C_5H_5)]$ (6b**).** This compound was prepared by a similar method to that used for the molybdenum analogue but with the use of [*n*-Bu₄N][W(CO)₃(η -C₅H₅)] (5.97 mmol) and (NPCl₂)₃ (3 g, 8.62 mmol). Chromatography gave WCl(CO)₃(η -C₅H₅) (240 mg) on elution with dichloromethane-hexane (1:5), identified by comparison of its carbonyl IR spectrum with that of an authentic sample. Further elution with dichloromethane-hexane (2:1) developed a pale yellow band which yielded yellow crystals of N₃P₃Cl₄(C₅H₅)[W(CO)₃(η -C₅H₅)] (1.15 g, 60%), mp 175 °C dec. Anal. Calcd for C₁₃H₁₀N₃Cl₄O₃P₃W: C, 23.12; H, 1.48; Cl, 21.01; N, 6.22; P, 13.78. Found: C, 23.18; H, 1.59; Cl, 21.57; N, 6.21; P, 14.27. Infrared peaks (KBr disk) detected (cm⁻¹): 2038 (s), 1963 (s), 1953 (s), 1930 (s) (ν_{CO}); 1194 (s), 1148 (s) (ν_{PN}); 517 (s), 454 (m), 416 (s) (ν_{PCl}); (in CH₂Cl₂ solution) 2036 (s) and 1948 (s, br) (ν_{CO}).

Reaction of [*n*-Bu₄N][Cr(CO)₃(η -C₅H₅)] with N₃P₃Cl₆ and MeI. A solution of [*n*-Bu₄N][Cr(CO)₃(η -C₅H₅)] (14.9 mmol), prepared as above, was added to a mixture of (NPCl₂)₃ (5.2 g, 14.95 mmol) and MeI (2.2 g, 15.5 mmol) dissolved in dichloromethane solution (50 mL) and was stirred at room temperature for 17 h. The products were separated by column chromatography. Elution with dichloromethane-hexane (1:5) gave CrI(CO)₃(η -C₅H₅) (1.85 g, 38%), identified by ¹H NMR and IR spectroscopy. Further elution with dichloromethane-hexane (1:5) gave N₃P₃Cl₅[Cr(CO)₃(η -C₅H₅)] (635 mg, 9%).

Reaction of [*n*-Bu₄N][W(CO)₃(η -C₅H₅)] with (NPCl₂)₃ and MeI. A solution of [*n*-Bu₄N][W(CO)₃(η -C₅H₅)] (9.01 mmol), prepared as described above, was added dropwise to a mixture of (NPCl₂)₃ (3.15 g, 9.05 mmol) and MeI (1.3 g, 9.15 mmol) dissolved in dichloromethane (50 mL) and was stirred for 17 h at room temperature. The reaction solvent was then removed under reduced pressure, and the products were separated by column chromatography. Elution with dichloromethane-hexane (1:9) gave a pale yellow band of WMe(CO)₃(η -C₅H₅) (1.78 g, 57%) identified by comparison of its ¹H NMR and carbonyl IR spectrum with those from an authentic sample. Further elution with dichloromethane-hexane (1:4) gave WCl(CO)₃(η -C₅H₅) (336 mg, 10.1%) identified by comparison of its carbonyl IR spectrum with an authentic sample. Elution with dichloromethane-hexane (1:1) gave first N₃P₃Cl₄(C₅H₅)[W(CO)₃(η -C₅H₅)] (216 mg, 7.1%) followed by a yellow band which yielded pale yellow crystals of N₃P₃Cl₄Me[W(CO)₃(η -C₅H₅)] (175 mg, 3.1%), mp 210 °C dec. Anal. Calcd for C₆H₈N₃Cl₄O₃P₃W: C, 17.30; H, 1.29; N, 6.73. Found: C, 16.86; H, 1.45; N, 6.46. Infrared peaks (KBr disk) (cm⁻¹): 2033 (s), 1961 (s),

1930 (s, br) (ν_{CO}); 1200 (s), 1165 (s), 1151 (s) (ν_{PN}); 567 (s), 503 (s), 434 (s) (ν_{PCl}); (in CH₂Cl₂ solution) 2035 (s), 1957 (sh), 1942 (s) (ν_{CO}).

Single-Crystal X-ray Data Collection. Suitable crystals of **5**, **6a**, and **6b** were obtained as yellow, transparent parallelepipeds from dichloromethane-hexane solution. The crystal dimensions and other X-ray data are listed in Table VI. The general X-ray data-collection technique was the same as reported in our recent publications.²

Single-Crystal X-ray Data Collection. Suitable crystals of **5** were obtained as bright yellow, transparent parallelepipeds from dichloromethane-hexane solution. A single, well-formed example of dimensions ca. 0.25 × 0.25 × 0.18 mm was chosen for analysis and was mounted on a glass fiber along the longest axis. The crystal was mounted in a random orientation on an Enraf-Nonius CAD4 diffractometer, optically centered, and 25 reflections were located. Least-squares refinement of the reflections indicated a monoclinic lattice of dimensions $a = 8.334$ (3) Å, $b = 12.897$ (8) Å, $c = 8.783$ (4) Å, $\beta = 105.44$ (3)°, $V = 909.9$ (15) Å³, with $Z = 2$ for a $\rho_{\text{calcd}} = 1.87$ g/cm³.

Intensity data were measured for 1792 reflections ($3.0 < 2\theta < 44.0^\circ$) with use of single-crystal graphite-monochromated Mo K α radiation. From these, 1214 unique reflections were considered observed ($I > 2\sigma(I)$). A variable scan rate was employed from 1 deg/min for weak reflections to 4 deg/min for the most intense reflections. A variable angular scan width (ω) of (0.80 + 0.347 tan θ)° below and above the calculated $K\alpha_1$ and $K\alpha_2$ reflections was also used. Three standard reflections were measured every 2 h of actual X-ray exposure time and were used to place the data on a common scale (drift correction 0.995–1.213). No absorption corrections were applied ($\mu = 16.54$ cm⁻¹) since psi scans indicated that the absorption was not severe. The data were corrected for Lorentz and polarization factors and were used in the refinement of the structure. Inspection of the data set indicated that the space group was $P2_1/m$ (no. 11, C_{2h}^2).²⁸

Single well-formed examples of **6a** and **6b** having dimensions of 0.10 × 0.30 × 0.29 mm and 0.22 × 0.35 × 0.58 mm, respectively, were chosen and used in the X-ray analysis. Individual crystals were mounted as before on an Enraf-Nonius CAD4 diffractometer, optically centered, and 25 reflections were located. Least-squares refinement of the reflections indicated orthorhombic lattices having the following dimensions. **6a**: $a = 16.075$ (3) Å, $b = 8.832$ (3) Å, $c = 14.780$ (3) Å, $V = 2098$ (1) Å³, with $Z = 4$ for a $\rho_{\text{calcd}} = 1.858$, $\rho_{\text{meas}} = 1.854$ g/cm³. **6b**: $a = 16.053$ (2) Å, $b = 8.832$ (3) Å, $c = 14.755$ (4) Å, $V = 2092$ (1) Å³, with $Z = 4$ for $\rho_{\text{calcd}} = 2.142$, $\rho_{\text{meas}} = 2.120$ g/cm³.

Intensity data were measured on **6a** for 2851 reflections ($3.0^\circ < 2\theta < 55.8^\circ$) with use of single-crystal graphite-monochromated Mo K α radiation. From these, 1864 unique reflections were considered observed ($I > 2\sigma(I)$). A variable scan rate was employed from 1 deg/min for weak reflections to 5 deg/min for the most intense reflections. A variable angular scan width (ω) of (0.70 + 0.347 tan θ)° below and above the calculated $K\alpha_1$ and $K\alpha_2$ reflections was also used. Three standard reflections were measured every 2 h of actual X-ray exposure time and were used to place the data on a common scale (drift correction 0.935–1.037). No absorption corrections were applied ($\mu = 13.58$ cm⁻¹), since psi scans indicated that absorption was not severe. The data were corrected for Lorentz and polarization factors and were used in the refinement of the

(28) "International Tables for X-Ray Crystallography"; Kynoch Press: Birmingham, England, 1969, Vol. 1, p 99.

Table VIII. Positional and Thermal Parameters and Their Standard Deviations for **6a**

atom	x	y	z	U(1,1)	U(2,2)	U(3,3)	U(1,2)	U(1,3)	U(2,3)
Mo	0.25062 (6)	0.44715 (7)	0.0000 (0)	0.0314 (2)	0.0287 (2)	0.0246 (2)	0.0004 (4)	0.0030 (4)	-0.0006 (4)
C11	0.0977 (3)	0.9502 (4)	-0.0988 (2)	0.151 (3)	0.052 (2)	0.051 (1)	-0.031 (2)	-0.045 (2)	0.022 (1)
C12	-0.0421 (2)	0.9271 (4)	0.0402 (4)	0.044 (2)	0.078 (2)	0.180 (5)	0.023 (2)	-0.018 (2)	-0.027 (3)
C13	0.2859 (2)	0.9618 (4)	0.1916 (3)	0.084 (2)	0.054 (2)	0.106 (2)	-0.022 (2)	-0.056 (2)	0.005 (2)
C14	0.1175 (3)	0.9262 (4)	0.2886 (2)	0.148 (3)	0.071 (2)	0.038 (1)	0.052 (2)	0.002 (2)	-0.012 (2)
P1	0.1413 (1)	0.5867 (2)	0.0883 (2)	0.031 (1)	0.0223 (9)	0.027 (1)	0.001 (1)	0.001 (1)	0.000 (1)
P2	0.0755 (2)	0.8635 (3)	0.0246 (2)	0.039 (1)	0.026 (1)	0.042 (1)	0.003 (1)	-0.012 (1)	0.002 (1)
P3	0.1745 (2)	0.8670 (3)	0.1729 (2)	0.053 (1)	0.025 (1)	0.031 (1)	0.004 (1)	-0.011 (1)	-0.004 (1)
O1	0.2770 (3)	0.0995 (9)	-0.0311 (6)	0.043 (4)	0.027 (3)	0.036 (5)	-0.000 (3)	-0.010 (4)	-0.005 (3)
O2	0.2830 (5)	0.3480 (9)	0.2011 (5)	0.065 (5)	0.024 (3)	0.034 (4)	0.004 (4)	-0.023 (4)	0.003 (4)
O3	0.0816 (5)	0.3462 (10)	-0.0874 (6)	0.041 (4)	0.024 (3)	0.028 (3)	0.003 (3)	-0.006 (4)	0.003 (3)
N1	0.0803 (5)	0.6873 (8)	0.0223 (5)	0.068 (5)	0.039 (4)	0.072 (6)	0.009 (4)	0.004 (5)	-0.011 (4)
N2	0.1300 (6)	0.9659 (8)	0.0933 (6)	0.079 (5)	0.058 (4)	0.035 (4)	0.013 (4)	0.000 (4)	0.016 (4)
N3	0.1844 (5)	0.6938 (8)	0.1666 (6)	0.058 (5)	0.060 (5)	0.064 (5)	-0.008 (5)	-0.023 (4)	-0.008 (5)
C1	0.2668 (6)	0.226 (1)	-0.0176 (7)	0.034 (6)	0.043 (5)	0.048 (7)	0.002 (4)	0.006 (4)	-0.004 (5)
C2	0.2690 (6)	0.379 (1)	0.1297 (7)	0.048 (6)	0.043 (5)	0.030 (5)	0.014 (5)	0.002 (4)	0.009 (4)
C3	0.1434 (7)	0.383 (1)	-0.0522 (7)	0.046 (5)	0.035 (5)	0.035 (5)	0.012 (5)	0.010 (5)	0.004 (5)
C1P	0.3580 (7)	0.624 (1)	0.0085 (9)	0.063 (6)	0.050 (5)	0.044 (6)	-0.022 (5)	-0.001 (6)	0.002 (6)
C2P	0.2942 (7)	0.692 (1)	-0.0368 (8)	0.048 (6)	0.037 (5)	0.059 (6)	0.004 (5)	0.026 (5)	0.008 (5)
C3P	0.2816 (8)	0.612 (2)	-0.1151 (8)	0.070 (7)	0.085 (8)	0.041 (5)	-0.041 (6)	-0.014 (6)	0.034 (5)
C4P	0.3385 (8)	0.491 (2)	-0.1171 (9)	0.061 (7)	0.066 (7)	0.064 (7)	-0.010 (6)	0.038 (6)	-0.007 (7)
C5P	0.3859 (7)	0.500 (1)	-0.0392 (9)	0.040 (6)	0.055 (6)	0.071 (7)	0.006 (5)	-0.000 (6)	0.023 (6)
C11P	0.0706 (6)	0.470 (1)	0.1506 (6)	0.029 (4)	0.031 (5)	0.030 (4)	0.002 (4)	0.012 (4)	0.006 (4)
C12P	0.0662 (6)	0.317 (1)	0.1548 (7)	0.044 (5)	0.023 (4)	0.045 (5)	0.003 (4)	0.013 (5)	0.007 (5)
C13P	-0.006 (7)	0.272 (1)	0.2147 (8)	0.049 (6)	0.039 (5)	0.051 (6)	-0.001 (5)	0.013 (5)	0.007 (5)
C14P	-0.0367 (6)	0.394 (1)	0.2462 (9)	0.053 (5)	0.060 (6)	0.051 (5)	-0.004 (5)	0.033 (5)	0.022 (6)
C15P	0.0038 (7)	0.534 (1)	0.2107 (8)	0.045 (5)	0.044 (6)	0.060 (6)	0.005 (6)	0.015 (5)	0.002 (5)
H1	0.3806	0.6585	0.0656	0.0384					
H2	0.2631	0.7799	-0.0167	0.0384					
H3	0.2404	0.6355	-0.1612	0.0384					
H4	0.3441	0.4147	-0.1646	0.0384					
H5	0.4304	0.4314	-0.0211	0.0384					
H12	0.1025	0.2482	0.1230	0.0384					
H13	-0.0164	0.1695	0.2293	0.0384					
H14	0.3943	0.3943	0.2876	0.0384					
H15A	-0.0352	0.5982	0.1178	0.0384					
H15B	0.0277	0.5960	0.2603	0.0384					

structure. Inspection of the data set indicated that the space group was $Pca2_1$ (no. 29, C_{2v}^2).²⁸

A small test set of intensity data was also collected for C_{2v}^2 . Inspection indicated that this space group was also $Pca2_1$ (no. 29, C_{2v}^2).²⁸ Since all spectroscopic and crystallographic data indicated that **6a** and **6b** were analogous compounds, a full data set was not collected for **6b**.

Structure Determination and Refinement. **Compound 5.** All atoms, including hydrogen atoms, were located from Patterson and electron-density difference syntheses,²⁹ and their positional and thermal parameters were refined by full-matrix least-squares methods. In the final cycle, 123 parameters were refined including the positional parameters for all atoms and the anisotropic thermal parameters for the non-hydrogen atoms. The isotropic thermal parameters for the hydrogen atoms were fixed at $B = 5.0 \text{ \AA}^2$. The largest parameter shift was only 1% of that of its standard deviation. Convergence was achieved with $R = 0.054$ and $R_w = 0.056$.³¹ The final electron density difference map was smooth, with maxima and minima $\pm 0.24 \text{ e/\AA}^3$. Complex scattering factors corrected for anomalous dispersion were used.³⁰

Compound 6a. All atoms, including hydrogen atoms, were located from Patterson and electron-density difference syntheses. However, the hydrogen atoms were fixed in calculated positions during the later stages of refinement. In the final cycle, 243 parameters were refined by full-

matrix least-squares methods, including the positional and anisotropic thermal parameters of all non-hydrogen atoms. The largest parameter shift in this cycle was only 6% that of its standard deviation. Convergence was achieved with $R = 0.041$ and $R_w = 0.043$. Complex scattering factors corrected for anomalous dispersion were used.

Tabulation of X-ray Data. Interatomic distances and bond angles with their associated esd's of compounds **5** and **6a** are presented in Tables II and IV (supplementary material). Selected least-squares planes and interplanar angles are given in Tables III and V (supplementary material). The positional and thermal parameters are listed in Tables VII and VIII. Observed and calculated structure factors in Tables IX and X are available as supplementary material.

Acknowledgment. We thank the U.S. Army Research Office for the support of this work.

Registry No. **4**, 940-71-6; **5**, 91280-62-5; **6a**, 91280-63-6; **6b**, 91280-64-7; **10b**, 91280-65-8; $[n\text{-Bu}_4\text{N}][\text{Cr}(\text{CO})_3(\eta\text{-C}_5\text{H}_5)]$, 91266-18-1; $\text{K}[\text{Cr}(\text{CO})_3(\eta\text{-C}_5\text{H}_5)]$, 69661-90-1; $[\text{Cr}(\text{CO})_3(\eta\text{-C}_5\text{H}_5)]_2$, 12194-12-6; $n\text{-Bu}_4\text{NBr}$, 1643-19-2; $[n\text{-Bu}_4\text{N}][\text{Mo}(\text{CO})_3(\eta\text{-C}_5\text{H}_5)]$, 61618-13-1; $[n\text{-Bu}_4\text{N}][\text{W}(\text{CO})_3(\eta\text{-C}_5\text{H}_5)]$, 68914-56-7; $[\text{W}(\text{CO})_3(\eta\text{-C}_5\text{H}_5)]_2$, 12091-65-5; $[\text{Mo}(\text{CO})_3(\eta\text{-C}_5\text{H}_5)]_2$, 12091-64-4; $\text{Cr}(\text{CO})_3(\eta\text{-C}_5\text{H}_5)$, 32628-88-9; $\text{WMe}(\text{CO})_3(\eta\text{-C}_5\text{H}_5)$, 12082-27-8; $\text{WCl}(\text{CO})_3(\eta\text{-C}_5\text{H}_5)$, 12128-24-4.

Supplementary Material Available: Tables of bond lengths and angles, selected least-squares planes and interplanar angles, and observed and calculated structure factors for **5** and **6a**, a stereo ORTEP view of **5** and **6a**, and an illustration of the nonplanarity of the phosphazene ring in **5** (28 pages). Ordering information is given on any current masthead page.

(29) All programs used in the data collection reduction and refinement are part of the Enraf-Nonius Structure Determination Package, Enraf-Nonius, Delft, The Netherlands, 1975 (revised 1977).

(30) "International Tables for X-Ray Crystallography", 3rd ed.; Kynoch Press: Birmingham, England, 1969; Vol. II.

(31) $R_1 = \sum |F_o| - |F_c| / \sum |F_o|$; $R_2 = [\sum \omega(|F_o| - |F_c|)^2 / \sum \omega(F_o)^2]^{1/2}$.